SUPPLEMENTARY INFORMATION

Antigen-capturing nanoparticles improve the abscopal effect and cancer immunotherapy

Yuanzeng Min[1, 2, 3], Kyle C. Roche[1, 2, 3], Shaomin Tian[2, 4], Michael J. Eblan[1, 2, 3], Karen P. McKinnon[2, 4], Joseph M. Caster[1, 2, 3], Shengjie Chai[2, 5], Laura E. Herring[6], Longzhen Zhang[7], Tian Zhang[8], Joseph M. DeSimone[2, 4, 9, 10, 11, 12], Joel E. Tepper[1, 2, 3], Benjamin G. Vincent[2, 5], Jonathan S. Serody[2, 4, 5], Andrew Z. Wang[*1, 2, 3, 7]

[1]Laboratory of Nano- and Translational Medicine, Carolina Center for Cancer Nanotechnology Excellence, Carolina Institute of Nanomedicine, [2]Lineberger Comprehensive Cancer Center, [3]Department of Radiation Oncology, and [4]Department of Microbiology & Immunology, [5]Department of Medicine, University of North Carolina at Chapel Hill, Chapel Hill, North Carolina 27599, United States, [6]UNC Proteomics Core Facility, Department of Pharmacology, University of North Carolina, Chapel Hill, NC, USA, 27599, [7]Jiangsu Center for the Collaboration and Innovation of Cancer Biotherapy, Cancer Institute, Xuzhou Medical University, Xuzhou, Jiangsu, China, [8]Division of Medical Oncology, Department of Medicine, Duke University Medical Center, Durham, North Carolina 27710, United States, [9]Division of Molecular Pharmaceutics, Eshelman School of Pharmacy, and [10]Department of Chemistry, University of North Carolina, Chapel Hill, NC 27599, USA, [11]Department of Chemical and Biomolecular Engineering, NC State University, Raleigh, NC 27695, USA, and [12]Sloan-Kettering Institute for Cancer Research, Memorial Sloan-Kettering Cancer Center, New York, NY 10021, USA

* Corresponding author, Email: zawang@med.unc.edu

Table of Contents of Supplementary Information

Supplementary Fig. 11. Representative flow plots used to evaluate frequency of IFN-γ producing T cells taken from spleens of animals treated with AC-NPs and subsequently stimulated *ex vivo* with TDPAs.

Supplementary Fig. 12. AC-NPs enhance immunotherapy by promoting cancer specific immunity.

Supplementary Fig. 13. Neoantigens elicit T cell stimulation in animals treated with immunotherapy and AC-NPs following radiotherapy.

Supplementary Fig. 14. Comparison of AC-NP accumulation in APCs in nearby lymph nodes between AC-NP injected intratumorally following radiotherapy and TDPAs coated AC-NPs injected subcutaneously.

Supplementary Fig. 15. TDPAs coated AC-NPs enhance the efficacy of cancer vaccines in $CD8^+$ T cell dependent manner.

Supplementary Tables:

Supplementary Table 1. The capture of neoantigens and DAMPs by AC-NPs is dependent upon their surface chemistry.

			#PSMs/Sequest Score				
Classification	**Gene**	**Protein**	**mPEG AC- NPs**	**DOTAP AC-NPs**	**NH2 AC-NPs**	**PLGA AC-NPs**	**Mal AC-NPs**
Neoantigens	Actn4	Alpha-actinin-4		1/3		3/5	4/9
	Ap3d1	AP-3 complex subunit delta-1				3/8	
	Dag1	Dystroglycan				4/7	
	Eef2	Elongation factor 2		6/18		12/40	1/2
	Tubb3	Tubulin beta-3 chain		1/2		3/3	3/7
DAMPs	H2afx	Histone H2AX		3/6		20/31	2/2
	H2afz	Histone H2A.Z		3/6		15/28	2/2
	H3f3c	Histone H3.3C		1/3		15/34	1/1
	Hist1h1b	Histone H1.5		2/2		1/2	
	Hist1h1c	Histone H1.2		17/30	2/4	22/45	2/3
	Hist1h1d	Histone H1.3		15/26	2/4	23/47	2/3
	Hist1h1e	Histone H1.4		9/14	1/3	20/40	1/3
	Hist1h2ah	Histone H2A type 1-H	2/8	3/6		22/47	3/9
	Hist1h3a	Histone H3.1		1/2		13/30	1/1
	Hist1h3b	Histone H3.2		3/9		22/63	1/1
	Hist1h4a	Histone H4		2/2	1/3	72/140	4/9
	Hist2h2ab	Histone H2A type 2-B		2/4		15/24	1/2
	Hmgb1	High mobility group protein B1		26/74		8/16	
	Hsp90aa1	Heat shock protein HSP 90-alpha		6/13	9/25	13/29	5/11
	Hsp90ab1	Heat shock protein HSP 90-beta		6/11	9/25	13/24	5/13
	Hspa1a	Heat shock 70 kDa protein 1A		2/4		3/8	3/9
	Hspa4	Heat shock 70 kDa protein 4		2/3	2/4	1/0	

Note: Reported PSMs and Sequest Scores represent average values of two runs.

Supplementary Table 2. List of antibodies used in flow cytometric analysis.

Antibody	Clone	Fluorophore	Vendor
CD3	17A2	APC-eFluor® 780	eBioscience
CD4	RM4-5	Alexa Fluor® 488	BD Biosciences
CD4	GK1.5	PE-Cyanine7	eBioscience
CD8α	53-6.7	APC	BD Biosciences
CD8α	53-6.7	APC-eFlour780	eBioscience
CD11c	N418	PE-Cyanine7	eBioscience
CD25	PC61.5	PE	eBioscience
CD45	Clone: 30-F11	eFluor® 450,	eBioscience
CD45R (B220)	RA3-6B2	eFluor® 450	eBioscience
F4/80	BM8	PE-eFluor® 610	eBioscience
FOXP3	FJK-16s	PE-eFluor® 610	eBioscience
IFN-γ	XMG1.2	Alexa Fluor® 488	eBioscience
CD16/CD32 (Fc Block)	2.4G2		BD Biosciences

Supplementary Figures:

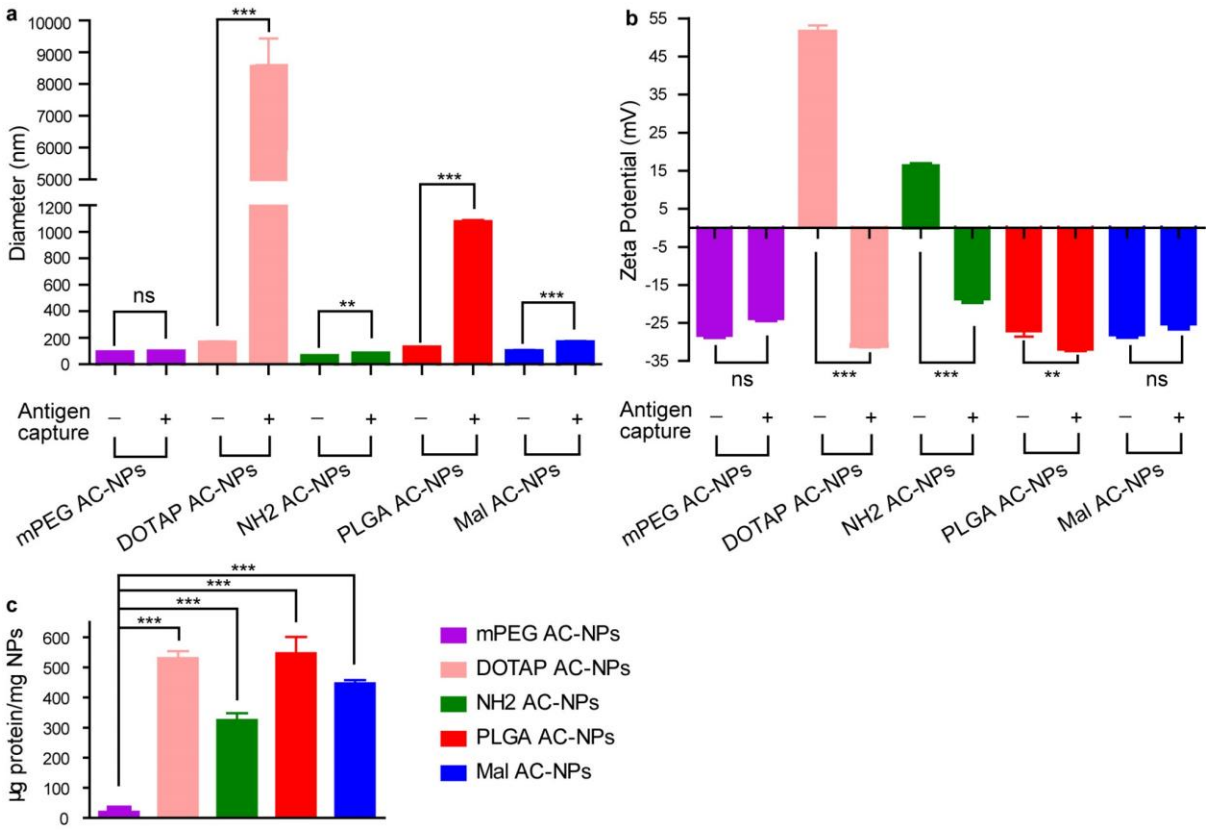

Supplementary Fig. 1. The size (a) and zeta potential (b) of AC-NPs change following antigen capture. (c) Quantification of protein captured by AC-NPs. The change in size and zeta potential of AC-NPs following capture and comparisons of total protein captured by AC-NPs were assessed by one-way analysis of variance (ANOVA) with Tukey's post-test. Data represent mean ±standard error of the mean (SEM). P value: *, $P<0.05$; **, $P<0.01$; ***, $P<0.005$.

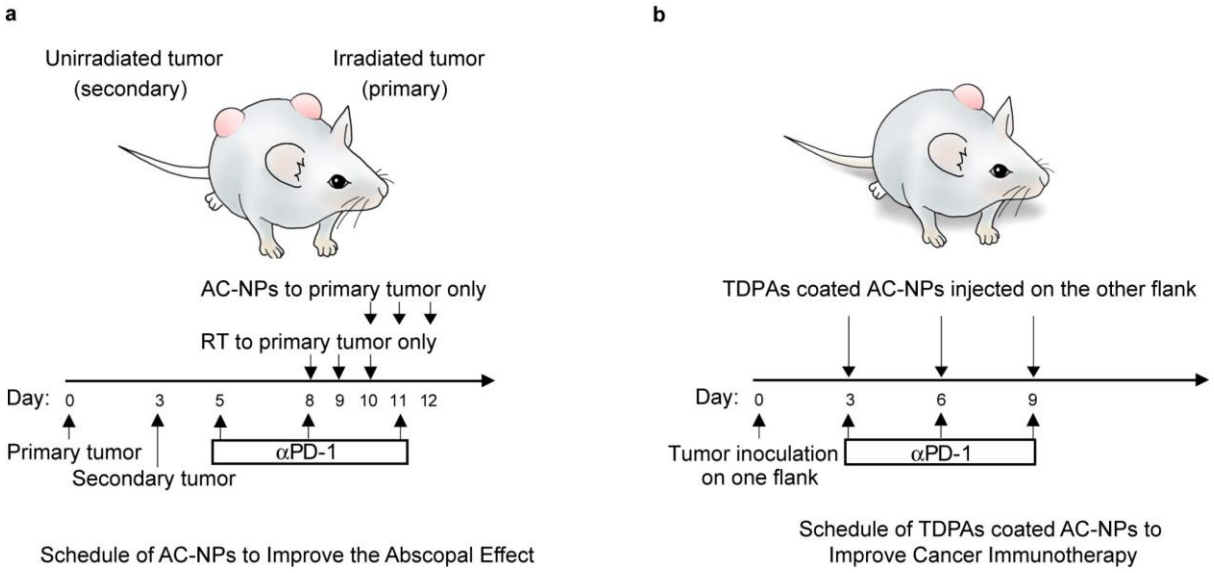

Supplementary Fig. 2. Schematics depicting the treatment timelines for *in vivo* cancer immunotherapy experiments. (a) The experimental approach used for *in vivo* assessment of AC-NP facilitated enhancement of immunotherapy and the abscopal effect following radiotherapy. (b) The experimental approach used for *in vivo* assessment of TDPA coated AC-NP with vaccine-based immunotherapy.

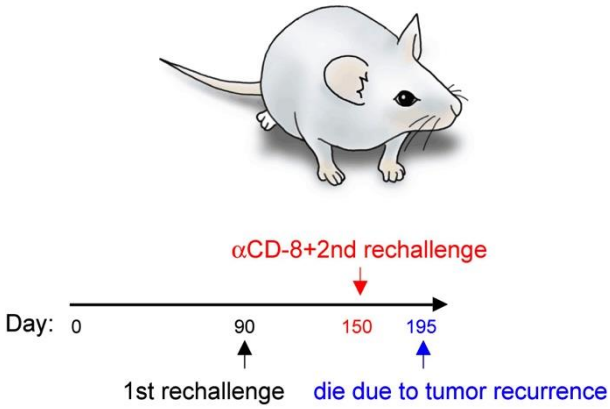

Supplementary Fig. 3. Animals demonstrating complete pathologic response following PLGA AC-NP+RT+anti-PD-1 treatment survived tumor re-challenge (subcutaneous injection of 100, 000 B16-F10 cells) (n=3). One animal was then again re-challenged while undergoing $CD8^+$ T cell depletion and failed to reject the tumor, requiring euthanasia due to tumor recurrence. (n=1)

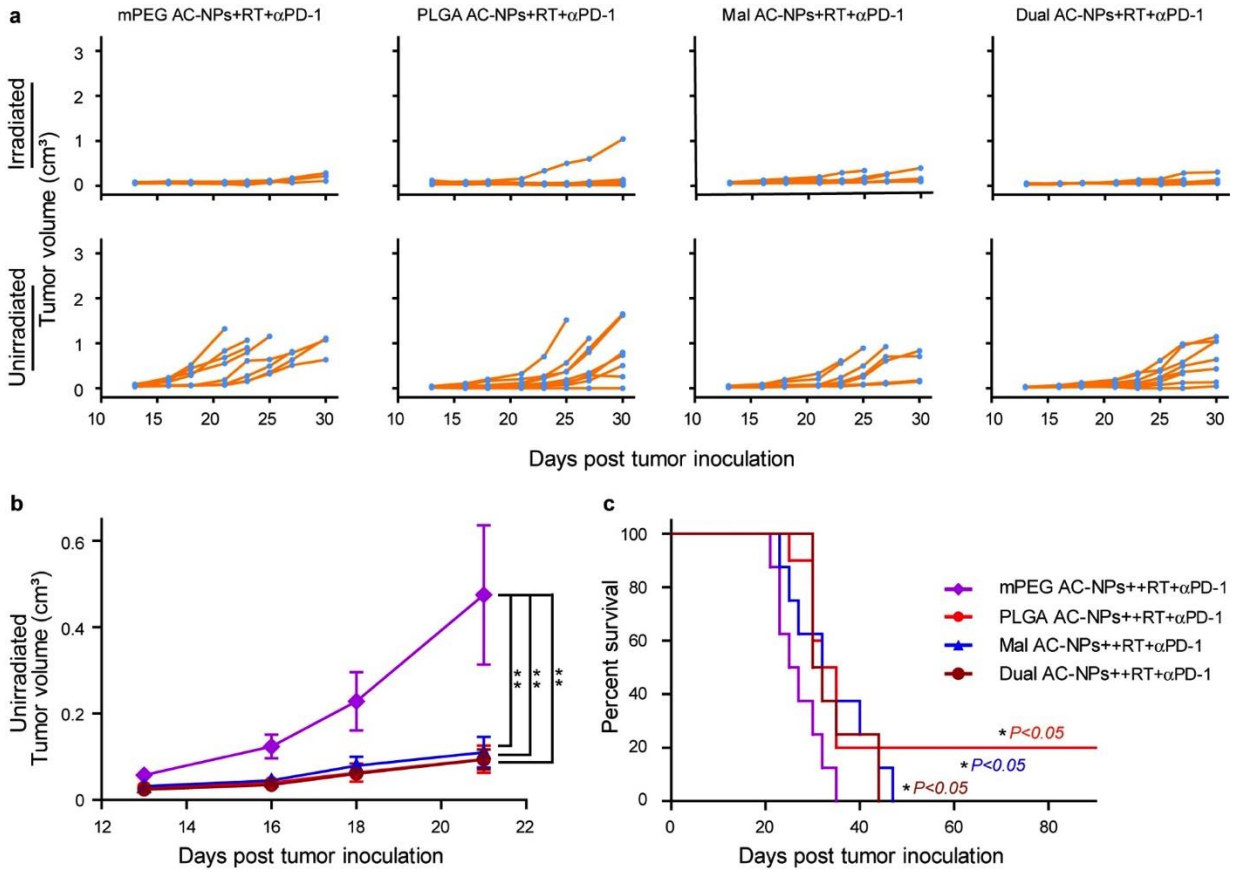

Supplementary Fig. 4. Mal and PLGA AC-NPs do not act synergistically to improve immunotherapy. (a) Tumor growth curves of individual animals treated with immunotherapy and AC-NPs. (b) Average tumor growth curves shown in (a). (c) Survival curves of mice in (a) (mPEG AC-NPs+RT+αPD-1, n=8; PLGA AC-NPs+RT+αPD-1, n=10; Mal AC-NPs+RT+αPD-1, n=8; Dual AC-NPs+RT+αPD-1, n=8). Tumor growth over time was compared by one-way analysis of variance (ANOVA) with Bonferroni correction. Data represent mean ± standard error of the mean (SEM). Differences in survival were determined for each group by the Kaplan-Meier method and the overall P value was calculated by the log-rank test. P value (*, P<0.05; **, P<0.01; ***, P<0.005)

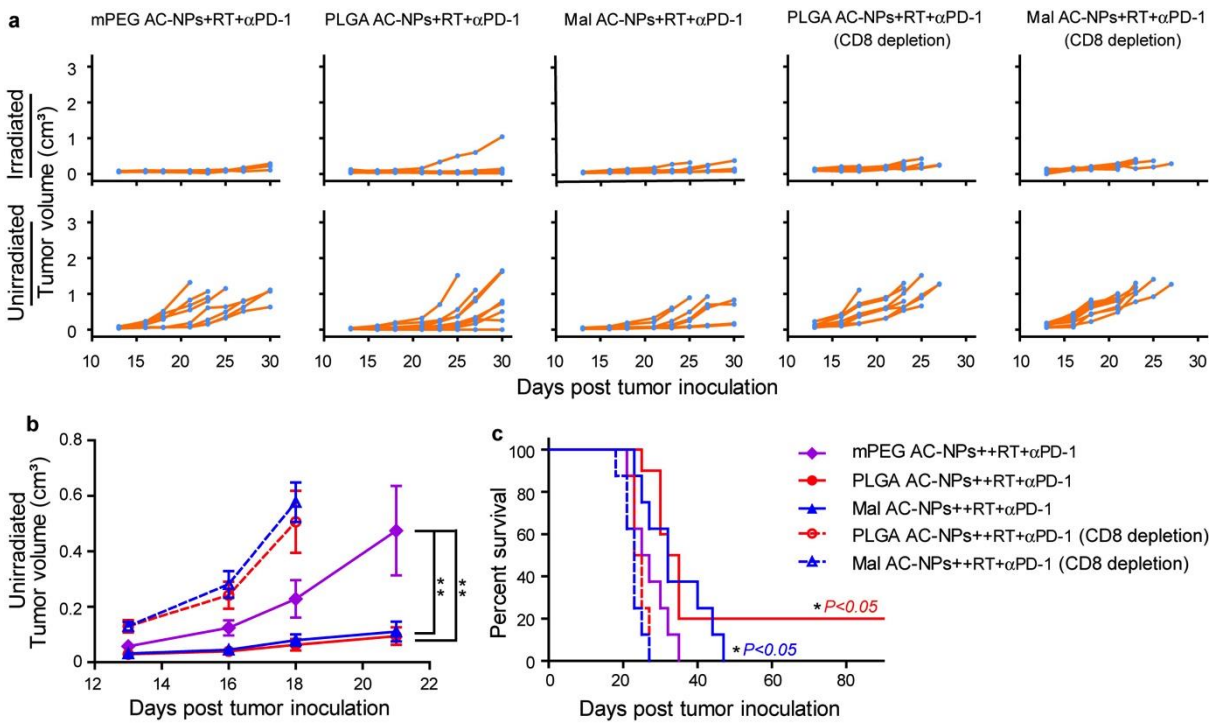

Supplementary Fig. 5. AC-NP facilitated enhancement of immunotherapy and the abscopal effect is lost following CD8+ T cell depletion. (a) Tumor growth curves of individual animals treated with immunotherapy and AC-NPs with or without CD8+ T cell depletion. (b) Average of tumor growth curves shown in (a). (c) Survival curves of mice in (a) (mPEG AC-NPs+RT+αPD-1, n=8; PLGA AC-NPs+RT+αPD-1, n=10; Mal AC-NPs+RT+αPD-1, n=8; PLGA AC-NPs+RT+αPD-1 (CD8 depletion), n=8; Mal AC-NPs+RT+αPD-1 (CD8 depletion), n=8). Tumor growth over time was compared by one-way analysis of variance (ANOVA) with Bonferroni correction. Data represent mean ± standard error of the mean (SEM). Differences in survival were determined for each group by the Kaplan-Meier method and the overall P value was calculated by the log-rank test. P value (*, P<0.05; **, P<0.01; ***, P<0.005)

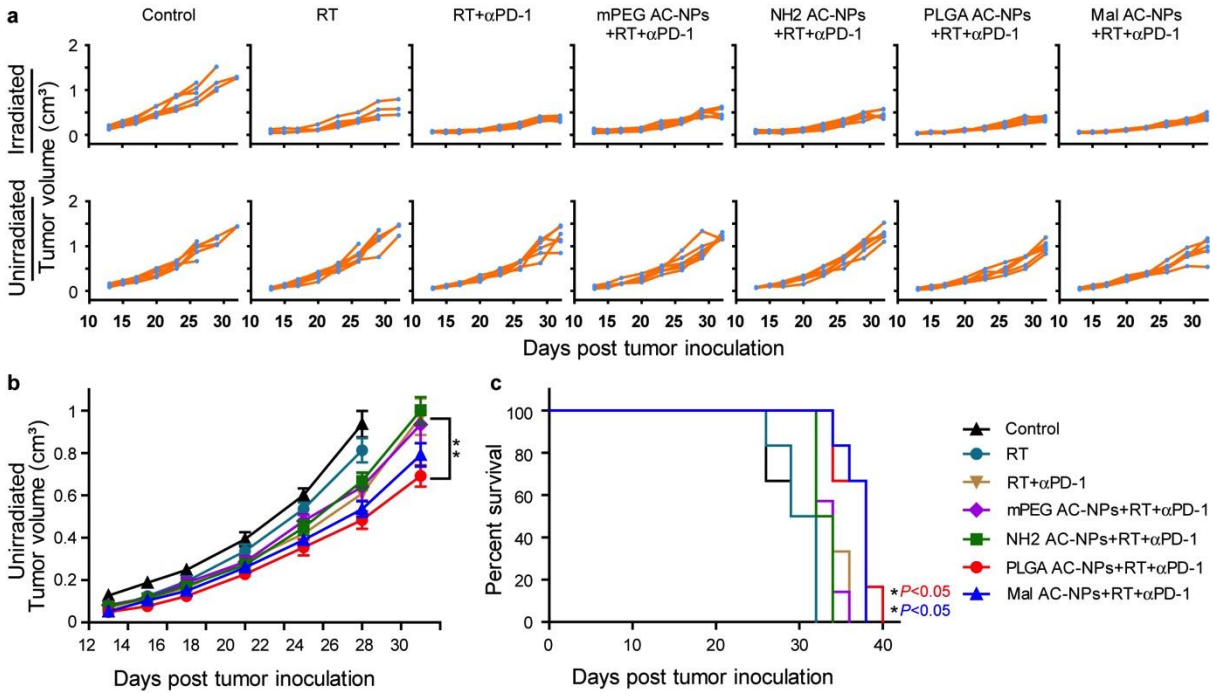

Supplementary Fig. 6. AC-NPs can improve immunotherapy and the abscopal effect in orthotopic 4T1 tumors. (a) Growth curves of irradiated (primary) and unirradiated (secondary) tumors in individual mice treated with immunotherapy and AC-NP formulations. (b) Average tumor growth curves of unirradiated (secondary) tumors in mice treated in (a). (c) Survival curves of the mice in (a). (n=6). Tumor growth over time was compared by the area under the growth curve (AUC). The difference was compared by one-way analysis of variance (ANOVA) with Dunnett's Multiple Comparison Test. Data represent mean ± standard error of the mean (SEM). Differences in survival were determined for each group by the Kaplan-Meier method and the overall *P* value was calculated by the log-rank test. *P* value (*, $P<0.05$; **, $P<0.01$; ***, $P<0.005$)

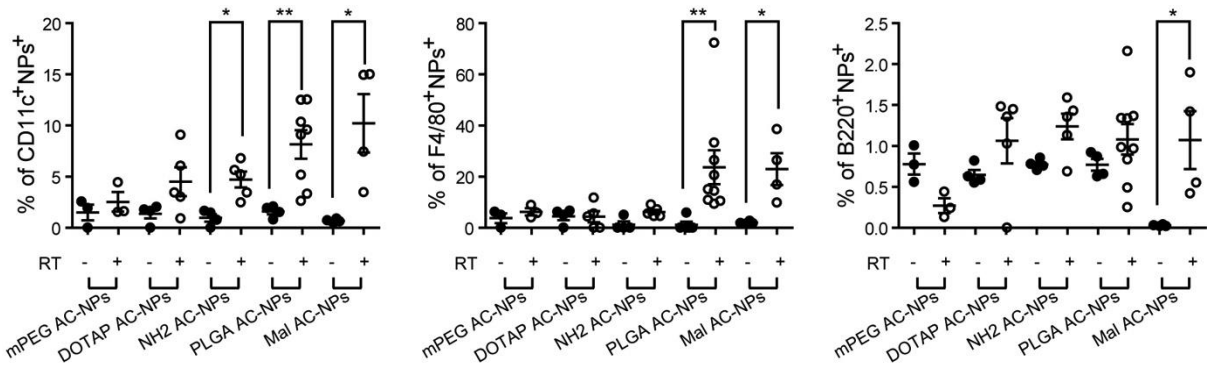

Supplementary Fig. 7. The accumulation of intratumorally injected AC-NPs in lymph node residing APCs is enhanced by radiotherapy. Flow cytometric analysis quantifying the percent of antigen presenting dendritic cells ($CD11c^+$), macrophages ($F4/80^+$), and B cells ($B220^+$) with fluorescently-labeled AC-NPs (mPEG AC-NPs, n=3; DOTAP AC-NPs, n=5; NH2 AC-NPs, n=5; PLGA AC-NPs, n=8; Mal AC-NPs, n=4). Statistical significance was assessed using Mann Whitney test. Data represent mean ±standard error of the mean (SEM). *P* value (*, $P<0.05$; **, $P<0.01$; ***, $P<0.005$)

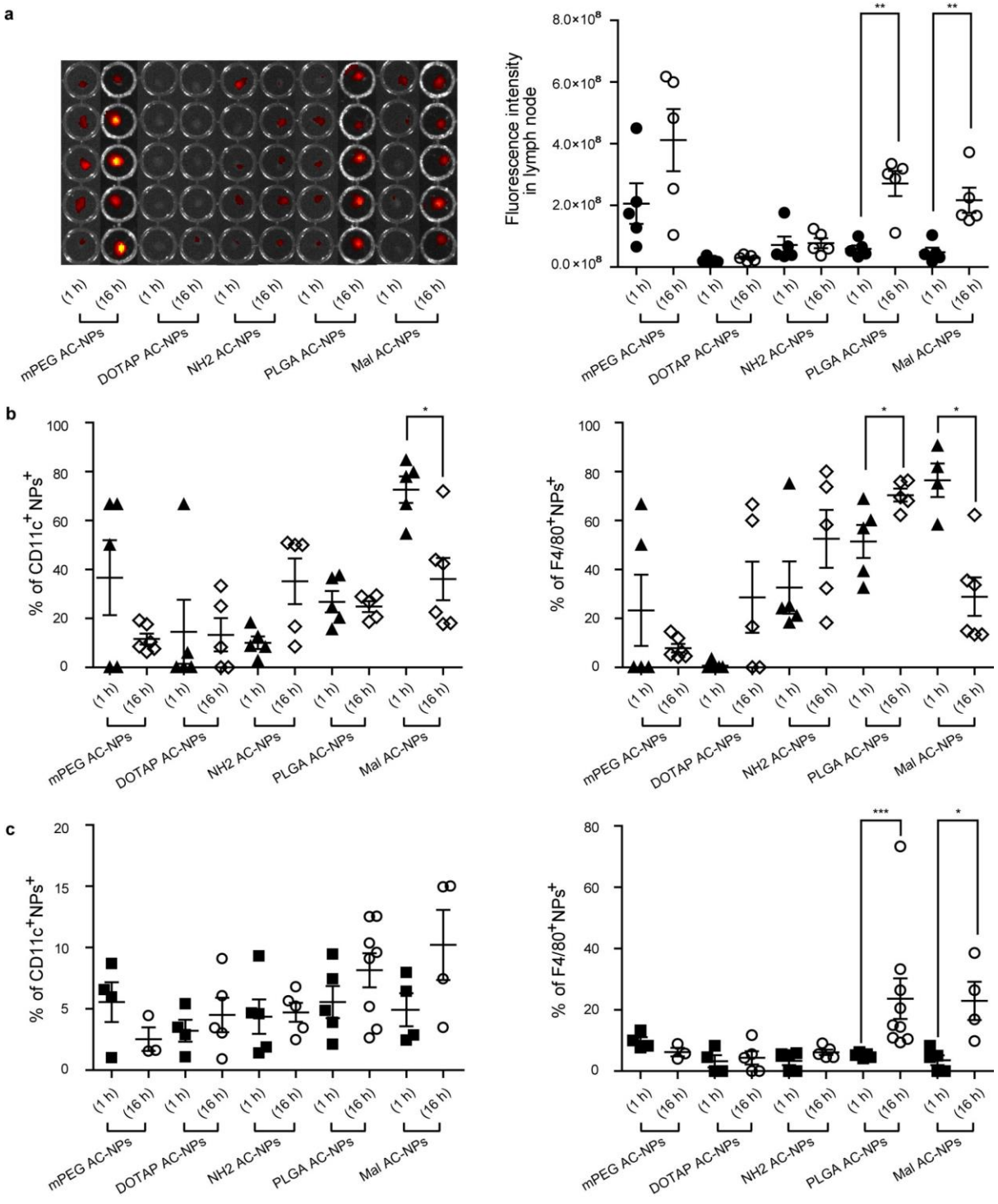

Supplementary Fig. 8. AC-NPs accumulate in APCs in the lymph node via cell mediated transport and cellular uptake following passive drainage after radiotherapy. (a) Images of sentinel lymph nodes at 1 and 16 hours after intratumoral injection of fluorescently-labeled AC-NPs, quantification of florescent intensity shown on the right (n=5). (b, c) Flow cytometric analysis assessing uptake of fluorescently labeled AC-NPs in dendritic cells ($CD11c^+$) and macrophages ($F4/80^+$) in irradiated tumors (b) and lymph nodes (c) (mPEG

AC-NPs, n=3-5; DOTAP AC-NPs, n=4-5; NH2 AC-NPs, n=5; PLGA AC-NPs, n=5 or 8; Mal AC-NPs, n=4). Statistical significance was assessed using Mann Whitney test. Data represent mean ±standard error of the mean (SEM). *P* value (*, $P<0.05$; **, $P<0.01$; ***, $P<0.005$)

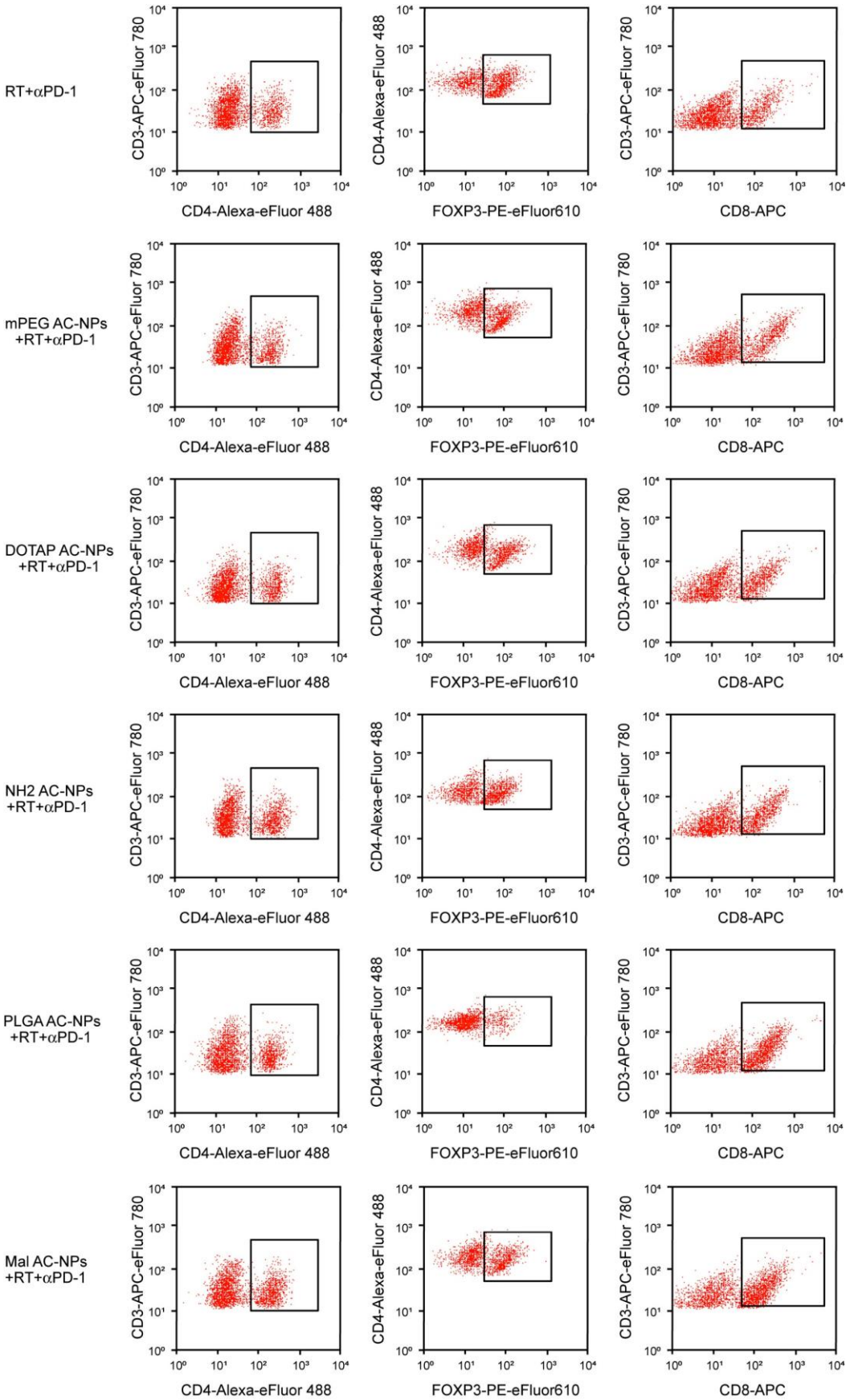

Supplementary Fig. 9 Representative flow plots used to quantify changes in the relative abundance of T cell subpopulations in unirradiated secondary tumors following treatment.

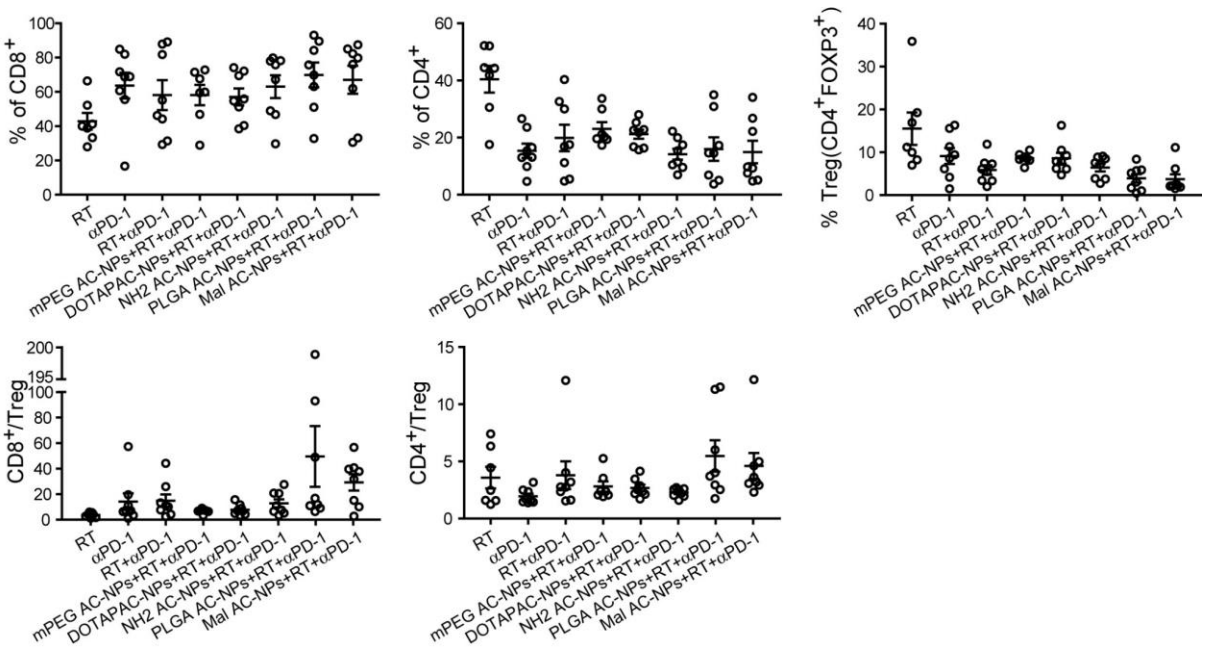

Supplementary Fig. 10 The effect of AC-NP administration on immune cell infiltrates within primary irradiated tumors. (a) Flow cytometric analysis assessing the relative abundance of $CD8^+$, $CD4^+$, and $CD4^+FOXP3^+$ T cell subpopulations in primary irradiated tumors (RT, n=7; αPD-1, n=8; RT+αPD-1, n=8; mPEG AC-NPs+RT+αPD-1, n= 7; DOTAP AC-NPs+RT+αPD-1, n= 8; NH2 AC-NPs+RT+αPD-1, n= 8; PLGA AC-NPs+RT+αPD-1, n= 8; Mal AC-NPs+RT+αPD-1, n=8). T cells were defined as being $CD45^+CD3^+$. Statistical significance was assessed using Mann Whitney test. Data represent mean ±standard error of the mean (SEM). *P* value (*, $P<0.05$; **, $P<0.01$; ***, $P<0.005$)

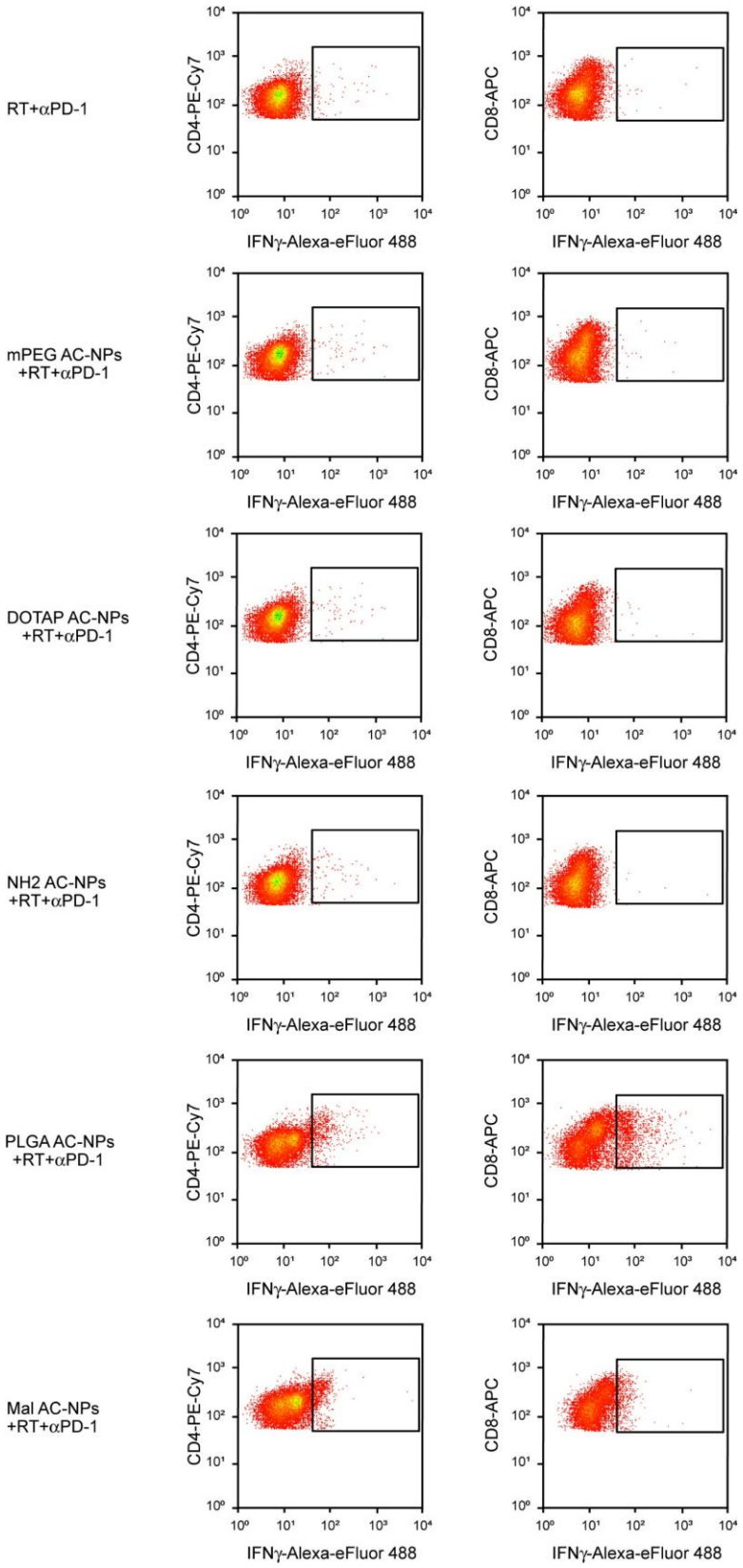

Supplementary Fig. 11 Representative flow plots used to evaluate frequency of IFN-γ producing T cells taken from spleens of animals treated with AC-NPs and subsequently stimulated *ex vivo* with TDPAs.

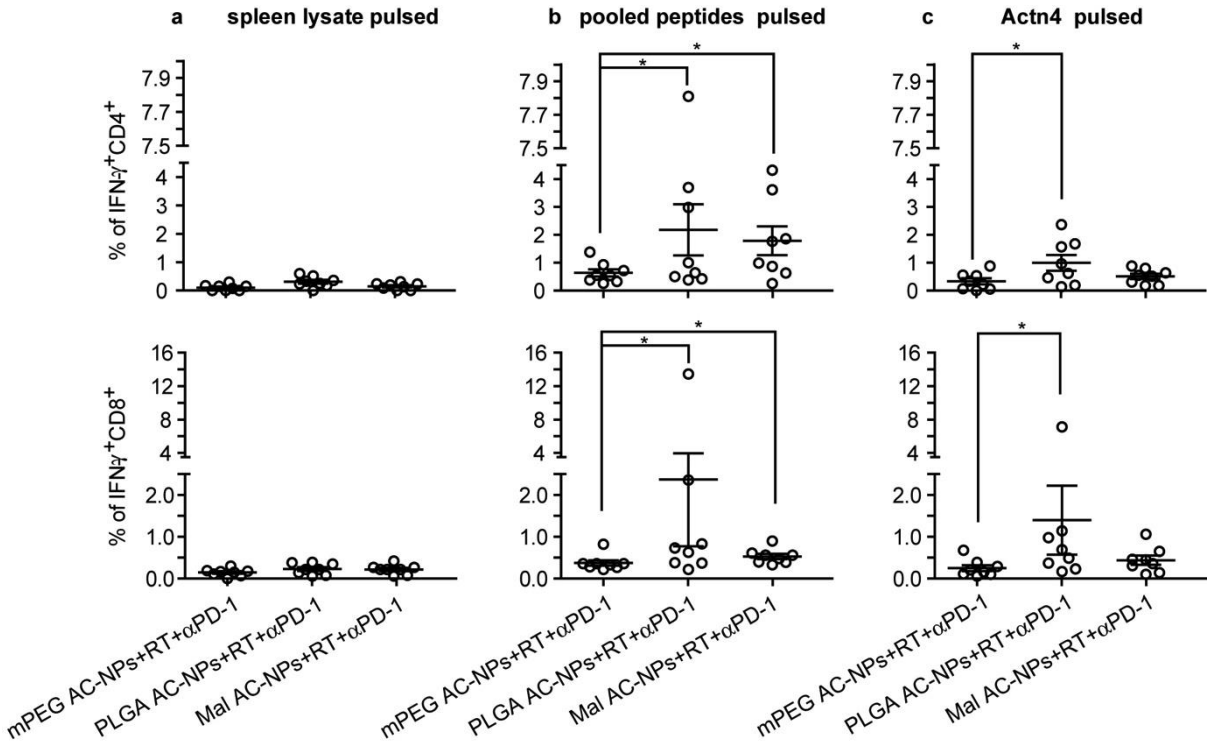

Supplementary Fig. 12 AC-NPs enhance immunotherapy by promoting cancer specific immunity. Flow cytometric analysis evaluating frequency of IFN-γ producing T cells taken from spleens of animals that underwent immunotherapy, intratumoral injection of AC-NPs following radiotherapy, and subsequently stimulated *ex vivo* with spleen lysates (a), pooled neoantigens (b), and the neoantigen Actn4 only (c). Note that the neoantigen pool consisted of Actn4, Tubb3, Dag1, and Eef2. (mPEG AC-NPs+RT+αPD-1, n= 8; PLGA AC-NPs+RT+αPD-1, n= 8; Mal AC-NPs+RT+αPD-1, n=8). Statistical significance was assessed using a Mann Whitney test. Data represent mean ±standard error of the mean (SEM). *P* value (*, $P<0.05$; **, $P<0.01$; ***, $P<0.005$)

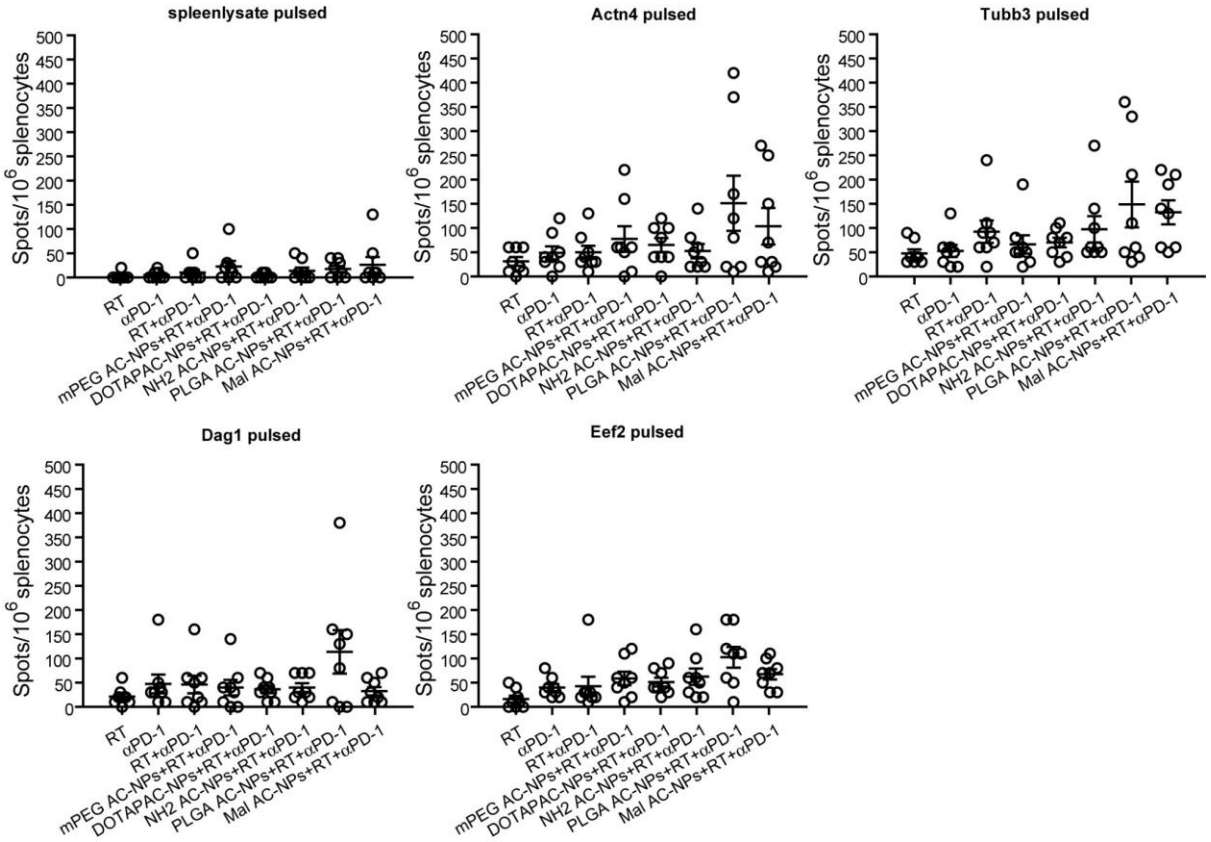

Supplementary Fig. 13. Neoantigens elicit T cell stimulation in animals treated with immunotherapy and AC-NPs following radiotherapy. Quantification of ELISPOT assay assessing IFN-γ production in splenocytes isolated from animals that underwent immunotherapy with or without intratumoral injection of AC-NPs following radiotherapy and subsequently stimulated *ex vivo* with normal spleen lysate, Actn4, Tubb3, Dag1 or Eef2 (n= 8). Statistical significance was assessed using Mann Whitney test. Data represent mean ±standard error of the mean (SEM). *P* value (*, $P<0.05$; **, $P<0.01$; ***, $P<0.005$)

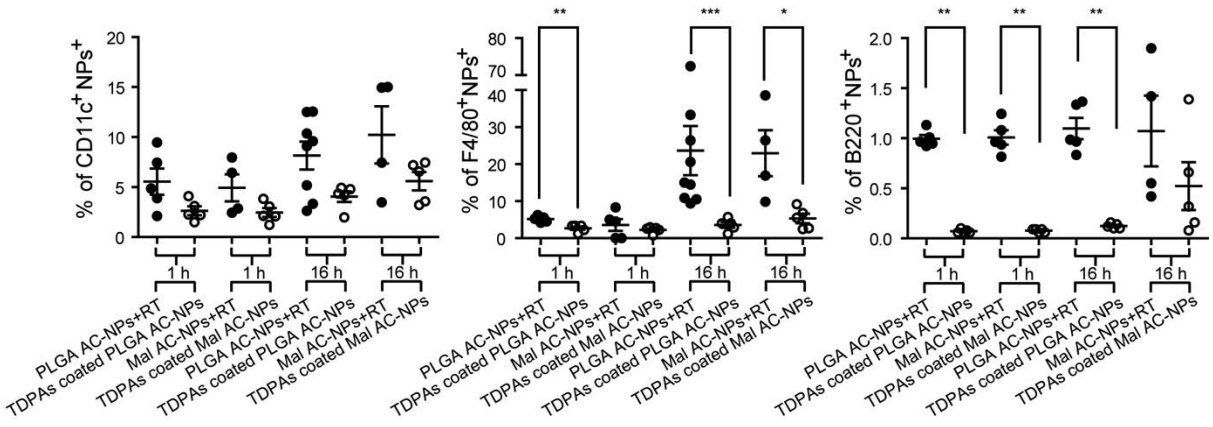

Supplementary Fig. 14. Comparison of AC-NP accumulation in APCs in nearby lymph nodes between AC-NP injected intratumorally following radiotherapy and TDPAs coated AC-NPs injected subcutaneously. Flow cytometric analysis assessing uptake of fluorescently labeled PLGA AC-NPs and Mal AC-NPs in dendritic cells ($CD11c^+$), macrophages ($F4/80^+$) and B cells ($B220^+$) (PLGA AC-NPs+RT, n=5-8; Mal AC-NPs, n=4-5; TDPAs coated PLGA AC-NPs, n=5; TDPAs coated Mal AC-NPs, n=5). Statistical significance was assessed using a Mann Whitney test. Data represent mean ±standard error of the mean (SEM). *P* value (*, $P<0.05$; **, $P<0.01$; ***, $P<0.005$)

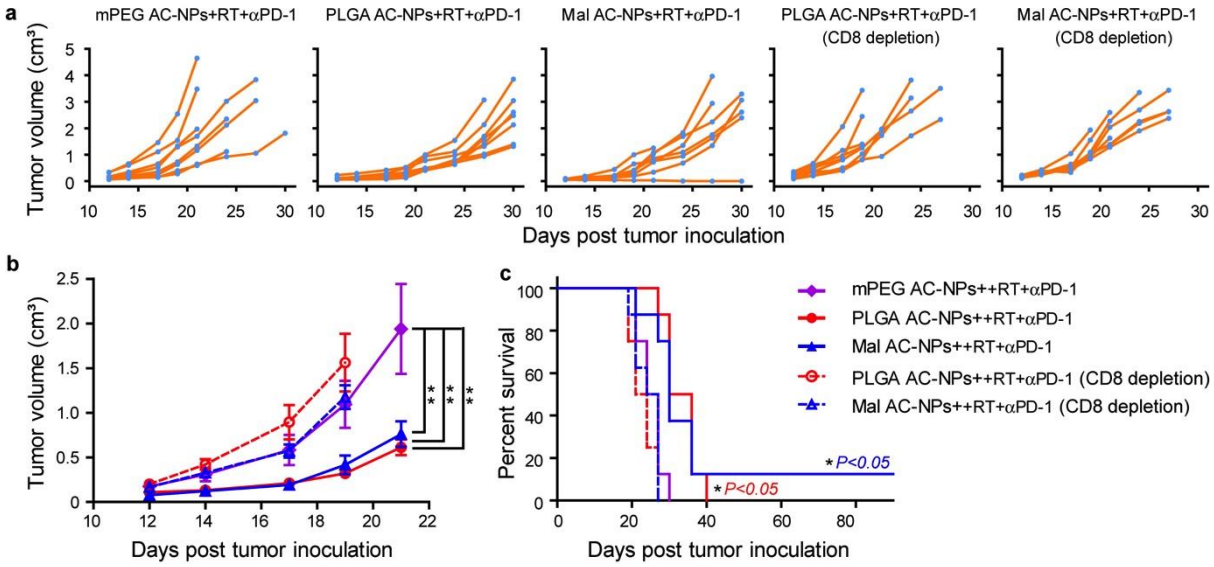

Supplementary Fig. 15. TDPAs coated AC-NPs act as cancer vaccines in a CD8+ T cell dependent manner. (a) Tumor growth curves of individual animals treated with immunotherapy and AC-NPs with or without CD8 depletion. (b) Average tumor growth curves shown in (a). (c) Survival curves of mice in (a) (n=8). Tumor growth over time was compared by one-way analysis of variance (ANOVA) with Bonferroni correction. Data represent mean ± standard error of the mean (SEM). Differences in survival were determined for each group by the Kaplan-Meier method and the overall P value was calculated by the log-rank test. P value (*, P<0.05; **, P<0.01; ***, P<0.005)